

Effect of $sp-d$ exchange interaction on excitonic states in CdSe/ZnSe/Zn_{1-x}Mn_xSe quantum dotsE. A. Chekhovich, A. S. Brichkin, A. V. Chernenko, and V. D. Kulakovskii
*Solid State Physics Institute, RAS, Chernogolovka, 142432, Russia*I. V. Sedova, S. V. Sorokin, and S. V. Ivanov
Ioffe Physico-Technical Institute, RAS, 194021 St. Petersburg, Russia

(Received 16 May 2007; revised manuscript received 15 July 2007; published 5 October 2007)

Photoluminescence of excitons (X) and biexcitons (XX) from single neutral CdSe/ZnSe/ZnMnSe quantum dots (QDs) with various magnitudes of $sp-d$ exchange interaction has been investigated in magnetic fields B up to 10 T at 1.8 K. The magnitude of the $sp-d$ interaction is varied by changing the penetration of the exciton wave function ψ_X into the diluted magnetic semiconductor (DMS) barrier, η , by variation of the nonmagnetic ZnSe barrier layer thickness about a value of 1.75 nm. The small penetration of ψ_X into the DMS barrier allowed a decrease of the X and XX emission line broadening caused by magnetic fluctuations and resolution of the fine structure of X states in a single QD. In contrast to bulk DMSs, the exciton line broadening when B is normal to the QD plane was found to be a nonmonotonic function of magnetic field: at high B it is suppressed due to Mn ion spin alignment, whereas at low B it is decreased due to the mixing of $J_z = +1$ and -1 X states in low-symmetry QDs by the electron-hole ($e-h$) exchange interaction. In addition, magnetic fluctuations result in (i) emission depolarization and enhanced splitting of exciton emission lines compared to the $e-h$ exchange interaction at $B=0$ and (ii) strong enhancement of spin relaxation between “bright” $J=1$ exciton states in magnetic fields normal to the QD plane already at $\eta \sim 1\%$. The spin relaxation from bright to “dark” exciton states is negligible up to $\eta \sim 4\%$. Auger recombination of excitons with excitation of Mn ions markedly decreases the quantum efficiency of exciton emission at $B=0$ already at $\eta \sim 4\%$.

DOI: [10.1103/PhysRevB.76.165305](https://doi.org/10.1103/PhysRevB.76.165305)

PACS number(s): 73.21.La, 75.75.+a, 78.55.Et

I. INTRODUCTION

Semiconductor quantum dots (QDs) with geometries smaller than or comparable to the bulk exciton Bohr radius represent a three-dimensionally (3D) confined system for electrons and holes. The full spatial quantization results in a discrete electronic energy spectrum resulting in the atomic-like character of the electronic states. The 0D behavior of these states has been confirmed in a large number of studies, using, e.g., optical spectroscopy of single quantum dots (SQDs) with a spatially resolved technique. The spatial resolution was achieved by defining a laterally constricted region by lithography,¹ by near-field scanning optical spectroscopy, and by exciting and/or detecting with a microscope objective.² The measurements showed that the QD exciton emission linewidth in both III-V and II-VI nonmagnetic semiconductor nanostructures is below 0.1 meV, which allows one to study the fine structure of QD exciton states caused by interparticle exchange interaction. The fine structure depends on the QD material, size and symmetry, the number of particles in the QD, external electric and magnetic fields, etc.^{3,4}

In this paper, we discuss the optical properties of states with one and two excitons in neutral II-VI QD structures doped with magnetic (Mn) ions of high density, so-called diluted magnetic semiconductors (DMSs) QDs. Strong $sp-d$ exchange interaction of Mn ions and free carrier spins in QDs can lead to a highly enhanced spin relaxation, giant Zeeman splitting of electron and hole states in a magnetic field, and formation of excitonic magnetic polarons, qualitatively changing the properties of QD confined excitons.⁵ Studies of individual neutral DMS QDs with large exchange interaction between charge carriers and Mn ions located in a

QD, or in barriers just near the QD,⁶⁻⁸ have shown that the observation of exciton fine structure in time-integrated spectra of individual QDs is highly obstructed by a strong emission line broadening due to thermal statistical fluctuations of the Mn magnetic moment. In DMS QDs with exciton energy exceeding internal electron transition energy in Mn ion one more problem appears, namely, the interaction with Mn ions leads to an additional highly effective nonradiative recombination channel absent in nonmagnetic QDs—Auger recombination of the exciton with energy transfer to Mn ions.^{9,10}

In order to avoid the problem of strong line broadening, Besombes *et al.*¹¹ used neutral CdTe QDs with single Mn ions. A well-pronounced fine structure connected to the $sp-d$ exchange interaction of the QD electron and hole with Mn ion spin has been observed. It has been found that this interaction can result in mixing of dark and bright exciton states.^{11,12} The influence of the $sp-d$ exchange interaction on the fine structure of bright exciton states in asymmetric QDs remains still undecided. The pure heavy-hole model used in these works is suitable for description of the magnetic field evolution of the emission spectra in symmetric QDs only, but it is inadequate for asymmetric ones.¹²

In this paper, we demonstrate that proper reduction of the exchange interaction strength through control of the electron and hole wave functions overlapping with Mn ions gives access to observation of the fine structure of bright exciton states in individual neutral DMS QDs. For that purpose, CdSe self-assembled quantum dots have been grown by molecular beam epitaxy on ZnSe and ZnMnSe cladding layers. The scheme of the structures studied is presented in Fig. 1. The CdSe QDs are separated from DMS Zn_{1-x}Mn_xSe barriers by additional nonmagnetic ZnSe layers. The $sp-d$ exchange interaction between spins of charge carriers and mag-

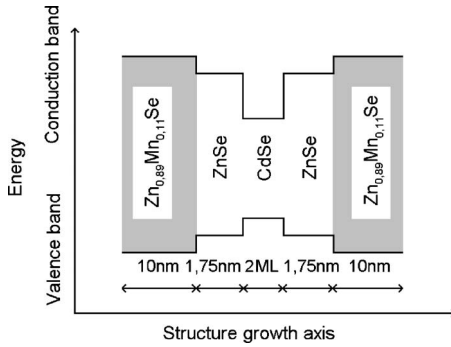


FIG. 1. Scheme of growth and energy bands of studied samples.

netic ions in DMSs is proportional to the square amplitude of the electron and hole wave functions at the point of the magnetic ion location.¹³ In CdSe/Zn_{1-x}Mn_xSe QDs, roughly half of the QD-localized electron and hole wave functions penetrate into the magnetic barrier, while in CdSe/ZnSe/Zn_{1-x}Mn_xSe structures the amplitude of electron and hole wave functions is reduced strongly in the nonmagnetic ZnSe layer.

Our studies have shown that the increase of the ZnSe layer thickness d up to 2.5 nm suppresses the $sp-d$ interaction almost completely. The small value of the intermixing between Mn and Zn atoms prevents the diffusion of Mn ions into QDs during the growth of the ZnSe spacer. Thus, the exchange interaction between exciton and Mn ions is controlled by the ZnSe barrier which strongly reduces the penetration of the exciton wave function into the Zn_{1-x}Mn_xSe layer, with Mn concentration chosen to be $x=0.11$, which gives maximum low-temperature magnetic susceptibility.

In our experiments, the thickness of the ZnSe layer has been chosen in the range 1.5–2 nm when the exchange interaction strength is, on one hand, strong enough to control the exciton properties studied but, on the other hand, results in line broadening not exceeding the exciton splitting due to electron-hole exchange interaction. Low-temperature photoluminescence (PL) measurements of excitons (X) and biexcitons (XX) from single neutral CdSe/ZnSe/Zn_{1-x}Mn_xSe QDs with various magnitudes of the $sp-d$ exchange interaction in magnetic fields normal and parallel to the QD plane have been used to study the effect of $sp-d$ exchange interaction on QD excitonic states in detail.

The paper is organized as follows. Experimental details are described in Sec. II. Section III is devoted to the description of emission spectra of QD excitons and biexcitons with various penetrations of the electron and hole wave functions into DMS barriers recorded in a wide range of magnetic fields up to 10 T in Faraday and Voigt geometries. The spin relaxation and Auger recombination of excitons in CdSe/ZnSe/Zn_{1-x}Mn_xSe QDs are discussed in Sec. IV. Section V describes the effect of $sp-d$ exchange interaction of QD excitons with Mn ion spins on exciton and biexciton transition energies. In Sec. VI we discuss the magnetic polaron formation process in QDs. In the last section we summarize the main features of QD excitons subjected to weak $sp-d$ exchange interaction with Mn ion spins. Finally, in the

Appendix we consider the energies, wave functions, and dipole transitions of excitons in CdSe/ZnSe/Zn_{1-x}Mn_xSe QDs.

II. EXPERIMENT

The samples investigated are CdSe self-assembled quantum dots grown by molecular beam epitaxy on ZnSe and Zn_{1-x}Mn_xSe cladder layers as shown in Fig. 1. The CdSe layer is separated from the DMS Zn_{0.89}Mn_{0.11}Se barrier by an additional nonmagnetic ZnSe layer of ~ 1.75 nm thickness.^{14,15}

PL studies were performed in a magnetic cryostat equipped with an optical window. The sample was immersed into pumped ⁴He at temperature 1.8 K. The light was collected in the direction normal to the QD layer. The external magnetic field was applied either perpendicular ($B \parallel Oz$, Faraday geometry) or parallel ($B \perp Oz$, Voigt geometry) to the sample plane. In order to obtain the signal from individual QDs, the sample surface was etched deeper than the QD layer everywhere, except for periodically arranged mesas of various sizes. The sample was excited by the ultraviolet line of an Ar ion laser ($\lambda=355$ nm), and the PL signal was analyzed by a monochromator combined with a charge-coupled device camera. It was found that the PL spectra obtained from individual mesas of size as small as ~ 150 – 250 nm provide emission lines from a relatively small number of individual QDs, so that some of them can be well resolved spectrally. The representative set of SQD emission spectra discussed below has been obtained from analysis of a large number of individual mesas in several samples.

In time-resolved studies, the sample was excited by the second harmonic of a pulsed picosecond Ti-sapphire laser ($\lambda=425$ nm), and the PL signal from individual mesas was analyzed by a monochromator combined with a streak camera with spectral and time resolution of ~ 1 meV and 25 ps, respectively.

III. EMISSION SPECTRA OF QD EXCITONS AND BIEXCITONS WITH VARIOUS PENETRATIONS OF CARRIER WAVE FUNCTION INTO DMS BARRIER

Figure 2 displays a typical set of emission spectra recorded at $T=1.8$ K in Faraday and Voigt geometries for individual QDs with different penetration¹⁶ η of the exciton wave function into the DMS barrier. In the spectrum of the QD with the lowest penetration of the exciton wave function into the DMS barrier displayed in Fig. 2(a), a doublet (marked X) with splitting ~ 250 μ eV at ~ 2.260 eV is observed at low excitation density $J=4J_0$ ($J_0=10$ W/cm²). Its components are cross-polarized along the $Ox' \parallel [110]$ and $Oy' \parallel [1\bar{1}0]$ directions. With increasing excitation density, a new doublet XX with a similar splitting but opposed order of components appears at energy ~ 2.236 eV. These are shown in Fig. 2(a) for $J=35J_0$. In an external magnetic field normal to the sample surface, splitting between components increases up to ~ 1 meV at $B=6$ T and their linear polarization gradually converts to circular one. Both doublets have the same order of σ^+ and σ^- components. Comparison to the emission spectra of nonmagnetic^{17,18} QDs shows that these

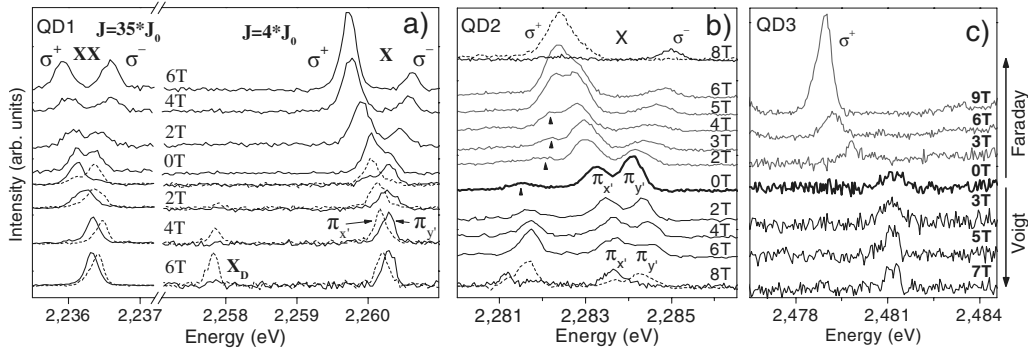


FIG. 2. Emission spectra of QDs with various amplitudes of exciton wave function in a DMS barrier in magnetic fields in Faraday and Voigt geometries at 1.8 K: (a) $\eta \sim 1\%$, (b) $\eta \sim 3\%$, and (c) $\eta \sim 4\%$. J denotes excitation power density, $J_0 = 10 \text{ W/cm}^2$. $\pi_{x'}$ and $\pi_{y'}$ correspond to linear polarization along $[110]$ and $[1\bar{1}0]$ directions, respectively.

features are characteristic for emission of an exciton (X) and biexciton (XX) recombination in QDs of low symmetry. Two X components polarized linearly in mutually perpendicular directions correspond to the emission of a bright (total spin $J=1$) exciton split by electron-hole exchange interaction due to a lowered QD symmetry. Two XX components correspond to the emission from a spin singlet XX state into the same doublet state of a single QD exciton. This explains the reverse order of linearly polarized $\pi_{x'}$ and $\pi_{y'}$ components.¹⁷

Figure 2(a) shows as well that a new highly polarized component appears in the QD exciton emission spectrum with increasing in-plane magnetic field $B \parallel O_y'$ about 2 meV below the emission of the bright exciton. Its intensity is proportional to $\sim B^2$. This line should be assigned to the emission from a dark, $J=2$, exciton state X_D as shown in the scheme in Fig. 3.³ Experiment shows that the relative intensity of this additional line changes strongly from one QD to another. This is well expected, as the emission from the dark exciton state is determined by the admixture of bright states caused by the magnetic field or QD symmetry lowering.

A more detailed comparison of emission spectra of CdSe/ZnSe/Zn_{1-x}Mn_xSe QDs and nonmagnetic CdSe/ZnSe

QDs in Refs. 17 and 18 shows that there are several differences caused by the effect of exchange interaction between QD carriers and Mn spins. These are (i) an increased line-width and its dependence on the magnetic field strength and direction, (ii) the opposite sequence of σ^+ and σ^- components compared to nonmagnetic QDs,¹⁹ (iii) sublinear dependence of their splitting on the magnetic field in Faraday geometry and the dependence of Zeeman splitting on temperature and excitation density, and (iv) enhanced spin relaxation of excitons. In particular, Fig. 4(a) displays emission spectra from QD1 recorded in a wide range of excitation densities from 10 to 350 W/cm^2 . An increasing excitation density leads to a strong growth of occupation of the excited state caused by the heating effect of the exciting beam and, in addition, to a well-pronounced decrease of Zeeman splitting. The latter is connected with diminution of the magnetic moment in the region of the exciton wave function due to heating of the Mn ion system. The dependences of the Zeeman splitting for two excitation densities in the whole range of magnetic fields are shown in Fig. 5(a).

Figures 2(b) and 2(c) illustrate the magnetic field behavior of spectra for QDs with larger parts of the exciton wave

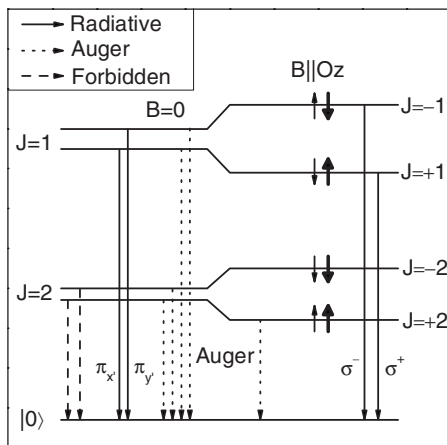


FIG. 3. Scheme of exciton energy levels and transitions in zero magnetic field and in high magnetic field in Faraday geometry. Short thick arrows correspond to the heavy-hole states with $j_{hz} = +3/2$ (arrow up) and $-3/2$ (arrow down); thin arrows correspond to electron states with $s_z = \pm 1/2$ (up and down arrows).

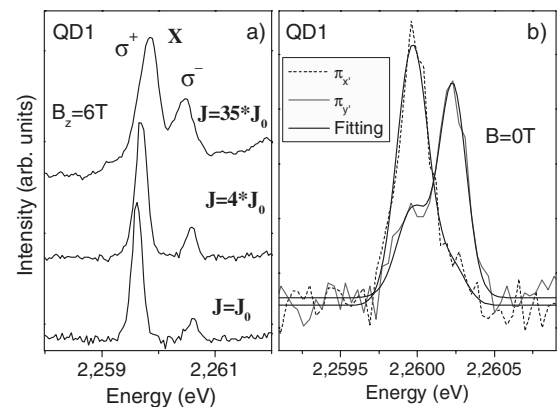


FIG. 4. (a) PL spectra of QD1 in Faraday geometry at $B=6 \text{ T}$ for different excitation power densities J ($J_0 = 10 \text{ W/cm}^2$). Spectra are normalized to the intensity of the low-energy component. (b) PL spectra of QD1 at field $B=0$ recorded in two linear polarizations along the main axes. Solid lines show the approximation of the spectra with two Gaussians.

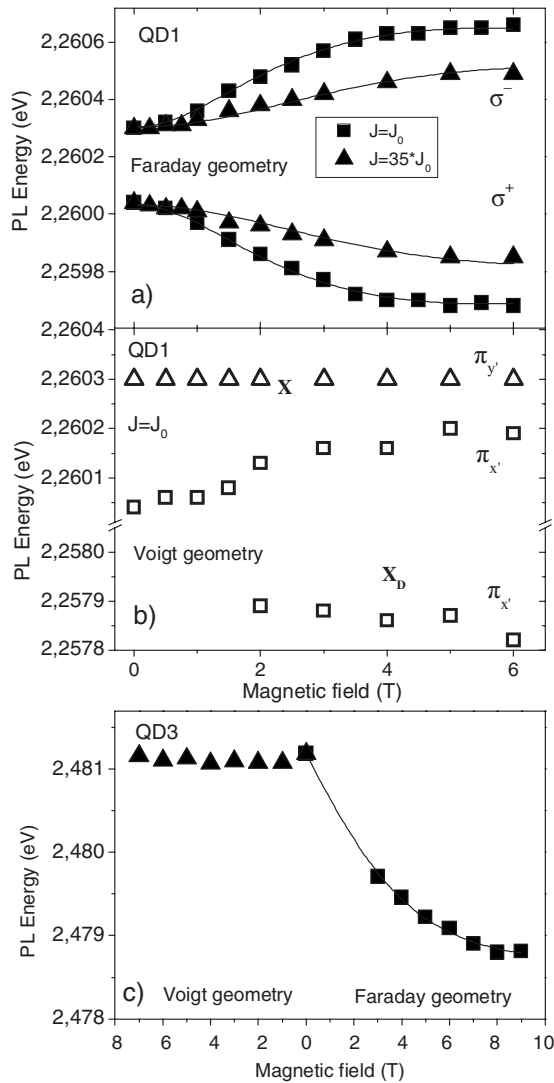


FIG. 5. Magnetic field dependence of PL energy obtained by fitting spectra showed in Fig. 2 with Gaussian curves for different excitation power J ($J_0=10$ W/cm²): (a) QD1 in Faraday geometry, (b) QD1 in Voigt geometry, and (c) QD3 in both Faraday and Voigt geometries. Solid lines are results of approximation.

function η in the DMS barrier. First, it is seen that an increase in η results in a further line broadening and in growth of the Zeeman splitting of the exciton doublet when $B \parallel O_z$. Second, the emission intensity from the excited $J_z=-1$ spin state of the bright exciton, $I_{U,1}$, decreases strongly with increasing η , indicating the acceleration of spin relaxation. Figure 2(c) shows that the emission from an excited bright exciton state disappears from the spectra in QD3 with $\eta \sim 0.04$. Finally, at $\eta \sim 0.04$ a strong decrease of the quantum efficiency of exciton emission is observed at $B=0$. An in-plane magnetic field does not change the quantum efficiency, whereas the high magnetic field $B \parallel O_z$ enlarges the exciton emission. The strong dependence of the quantum efficiency on the magnitude and direction of the magnetic field is characteristic for excitons in DMSs with energy gap exceeding the energy of the internal transition (~ 2.1 eV) between 6A_1 and 4T_1 states in the Mn ion. It is connected to effective

Auger recombination of an exciton with excitation of an electron in the d shell of Mn ions.^{9,10}

Comparison of the spectra in Figs. 2(a)–2(c) shows that the richest structure is observed in the emission spectrum from a low-symmetry QD with a middle value of $\eta \sim 0.03$ (QD2) displayed in Fig. 2(b). This QD reveals weak emission from a dark exciton state even at $B=0$, indicating that the QD symmetry is lower than C_2 . The lowering of the symmetry can be caused either by the low QD symmetry itself or by transverse magnetic fluctuations. Measurements on different QDs in the same sample with a similar η show that the relative intensity of dark exciton emission changes strongly from one QD to another. Thereby we connect the appearance of the dark exciton emission with the anisotropy of the QD rather than with magnetic fluctuations. The emission line of the dark exciton is located about 2 meV below the bright state, similar to that in QD1 with smaller η in Fig. 2(a). Zeeman splitting of exciton components for $B \parallel O_z$, enhanced due to $sp-d$ interaction, leads to the intersection of high-energy dark and low-energy bright exciton states at a relatively low $B \sim 5$ T. Figure 2(b) shows that the approach of the dark component to the bright one is followed by a strong growth of its intensity, indicating that the dark component borrows oscillator strength from the bright one due to coupling between them. At the crossing point, a well-pronounced repulsion of the two components with a coupling constant of ~ 0.2 meV and the exchange of their oscillator strengths are observed.

Similar coupling has been observed earlier by Besombes *et al.* in CdTe/ZnTe QDs with a single Mn ion in a QD.¹¹ They found a well-pronounced anticrossing between the states with a similar total spin of exciton and Mn ion, and attributed that to the coupling of the dark ($J_z=2$) and bright ($J_z=1$) heavy-hole exciton states via the electron-Mn-ion part of the interaction Hamiltonian. This coupling corresponds to a simultaneous electron and Mn-ion spin flip, changing a bright exciton into a dark exciton. A coupling constant of ~ 0.1 meV has been found in CdTe QDs. In our experiments well-pronounced coupling has been observed only in those dots that demonstrate emission from the dark states already at $B=0$. Thereby we conclude that the electron-Mn-ion interaction in our QDs is still insignificant, and the lowering of QD symmetry is responsible for anticrossing of bright and dark states.

The emission spectra in Fig. 2(b) show that an in-plane magnetic field up to 8 T is still too small to change the splitting of dark and bright exciton states markedly, but leads to a well-pronounced increase of the relative intensity of the dark exciton emission, similar to that in QD1. Moreover, both Zeeman components of the dark exciton appear in the emission spectrum of this QD at high B . They have an orthogonal linear polarization which is resolved in magnetic fields above 8 T.

Finally, let us discuss the effect of magnetic fluctuations on the line broadening. As mentioned above, these fluctuations in DMS QDs result in a large, several meV, half-width of the exciton emission line at zero magnetic field.⁷ The suppression of the longitudinal fluctuations of the magnetic moment in a magnetic field normal to the QD plane leads to the corresponding monotonic line narrowing. In a magnetic field

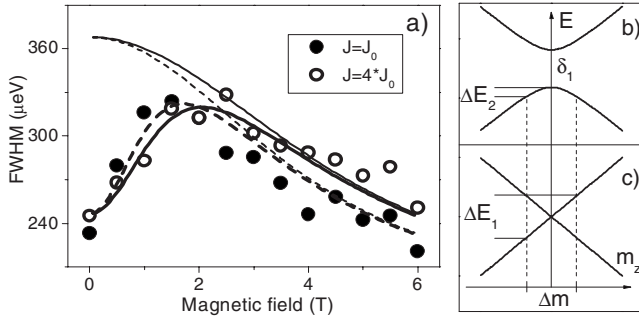


FIG. 6. (a) Magnetic field dependence of linewidth of exciton emission obtained by fitting spectra shown in Fig. 2 with Gaussian curves (symbols). The theoretical dependences are obtained from (A19) with (thick lines) and without (thin lines) account for e - h exchange splitting. Two different excitation densities are used: $J=J_0$ (closed symbols, dashed lines) and $J=4J_0$ (open symbols, solid lines); $J_0=10$ W/cm². The scheme of exciton energies at $B=0$ and $\vec{m} \parallel Oz$ with (b) and without (c) Faking account of anisotropic e - h exchange interaction. The fluctuation of Mn magnetization m_z in the range Δm leads to the broadening of the PL line $\sim \Delta E$, which is much greater in case (c), $\Delta E_1 > \Delta E_2$.

parallel to the QD plane the emission linewidth is controlled mostly by transverse magnetic fluctuations due to the strong anisotropy of the hole g factor. The decay of transverse fluctuations with magnetic field is slower than the decay of longitudinal ones. Thus the narrowing effect is less pronounced in this case.⁸

The magnetic field dependence of the full width at half maximum (FWHM) of X lines in QD1 is displayed in Fig. 6. It differs qualitatively from that in DMS QDs. The magnetic field dependence of the linewidth in QDs for $B \parallel Oz$ is a non-monotonic function of B : it increases at small B , reaches its maximum at $B \sim 2$ T, and only then decreases monotonically with B , similar to the behavior in DMS QDs.⁸ Such dependence is typical for both QD1 and QD2 and is observed both for exciton and biexciton emission. The reason for the non-monotonic magnetic field dependence of the FWHM will be discussed in Sec. V.

IV. SPIN RELAXATION AND AUGER RECOMBINATION OF EXCITONS IN CdSe/ZnSe/Zn_{1-x}Mn_xSe QDs

The spin relaxation in nonmagnetic CdSe QDs is very slow. In particular, the relaxation from the bright $J=1$ states to the lower-lying $J=2$ ones with spin flip of either electron or hole has a typical time of 10 ns, which greatly exceeds the radiative lifetime $\tau_{r,1}$ (~ 300 – 500 ps).^{20,21} As a consequence, the QDs are characterized by high quantum efficiency from the bright states. The characteristic time of simultaneous spin flip of the electron and hole in a QD, providing the scattering between two bright states, is much shorter, but also exceeds $\tau_{r,1}$.²² That leads to comparable intensities of the σ^- and σ^+ components in the emission of QD excitons even at Zeeman splitting $\Delta = g_z \mu_B B > kT$.

Figure 2(a) shows that, in the QD with a rather small ($\eta \sim 0.01$) penetration of the exciton wave function into the

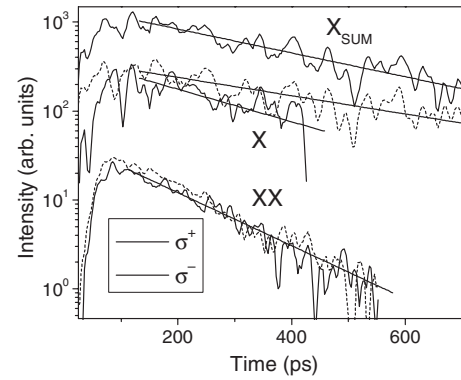


FIG. 7. Decay of Zeeman component emission of exciton (X), biexciton (XX), and total emission of exciton (X) in magnetic field $B_z=5$ T for a QD with low wave function penetration into a Zn_{1-x}Mn_xSe barrier, $\eta \sim 1\%$. Solid lines show approximation with monoexponential decay. Note that the XX and X_{sum} curves are shifted in vertical direction for the sake of clarity.

DMS barrier, the emission from the ground bright exciton state, $I_{G,1}$, remains strong in the whole range of magnetic fields both parallel and normal to the QD plane, similar to that in nonmagnetic QDs. Figure 2(c) shows that $I_{G,1}$ changes only in the QD with $\eta \sim 0.04$ (QD3). $I_{G,1}$ in this QD is large only at high magnetic fields normal to the QD plane. With decreasing magnetic field $I_{G,1}$ diminishes strongly and remains weak in the whole range of B parallel to the QD plane. In contrast, the emission intensity from the upper bright exciton state, $I_{U,1}$, decreases strongly in magnetic field $B \parallel Oz$ and at low excitation density.

The decreased emission from bright exciton states in CdSe QDs with DMS barriers can have two causes. These are (i) spin relaxation into the lower states and (ii) Auger recombination of excitons with excitation of a Mn ion from the ground 6A_1 state to the excited 4T_1 . The Auger recombination rate depends strongly on the spin states of both the exciton and the Mn ion: It is highly effective at low magnetic fields but becomes forbidden for bright excitons in high magnetic fields $B \parallel Oz$, due to the spin projection conservation law, when Mn ions are in the ground $S_{z,Mn} = -5/2$ spin state. In this case there remains only one allowed Auger transition—from the dark $J_z = +2$ state shown in the scheme in Fig. 3.⁹

The decay times of biexciton and bright exciton emission in QDs with $\eta \sim 0.01$ have been determined from the time-resolved spectra recorded with ~ 25 ps time resolution under excitation with 1.5 ps pulses. Figure 7 shows the time dependences of intensity of X and XX line at $B_z=5$ T. As expected, both XX components corresponding to the transition from the singlet XX state decay with a common time τ_{XX} . The analysis of temporal dependencies of the intensity gives the estimate for $\tau_{XX} \approx 140 \pm 20$ ps. Figure 7 shows as well that the decay of the total intensity of two exciton components can be described by an exponent with $\tau_X \approx 350 \pm 100$ ps. The values of τ_{XX} and τ_X are very similar to biexciton and bright exciton lifetimes in nonmagnetic CdSe/ZnSe QDs of similar size [$\tau_X \sim 300$ – 500 ps (Ref. 21)]. Therefore one can conclude that the penetration of the

exciton wave function into the magnetic barrier in these QDs is sufficient to cause neither marked Auger recombination of QD excitons with a excitation of Mn ions, nor relaxation to the lower-lying nonradiative $J=2$ state.

The measurements of the decay times of σ^+ and σ^- exciton components show that the upper, σ^- , component decays notably faster than the σ^+ component. The smaller value of τ_X^- indicates a marked spin relaxation from the upper spin state that is not characteristic for nonmagnetic CdSe/ZnSe QDs. The direct determination of the spin relaxation time from time-resolved measurements is obstructed as the pulse heats the QD. As long as the initial temperature after pulse is comparable to or exceeds the splitting of bright exciton states, the dynamics of the population is affected by thermal excitation from the ground spin state and hence does not correspond to a pure longitudinal spin relaxation time.

As Auger recombination of bright exciton in QDs with $\eta \sim 0.01$ is negligible, the small relative intensity from the excited component of the bright exciton, $I_{U,1}/I_{G,1}$, at high B should be connected to the effect of Mn ions on the spin relaxation from the excited $J_z=-1$ to the ground $J_z=+1$ state. Neglecting the slow spin relaxation to the dark states, one can estimate the ratio $\tau_{s,1}/\tau_X$ from the ratio $I_{U,1}/I_{G,1} = [2 \exp(-\Delta/kT) + \tau_{s,1}/\tau_X] / (2 + \tau_{s,1}/\tau_X)$. At $\Delta \gg kT$ the ratio $I_{U,1}/I_{G,1}$ tends to $\tau_{s,1}/(2\tau_X + \tau_{s,1})$. The temperature T depends on the excitation density. This is illustrated in Fig. 4(a), displaying exciton emission spectra from QD1 under cw excitation at $B_z=6$ T ($\Delta \sim 1$ meV) in a wide range of $J = 10-350$ W/cm². The figure shows that the emission from the $J_z=-1$ state disappears as J decreases down to 10 W/cm², when the effective temperature approaches that of the bath, $T_b=1.8$ K $\ll \Delta$. In this case the ratio $I_{U,1}/I_{G,1} \approx 0.14$, which gives $\tau_{s,1}/\tau_X \approx 0.32$, and hence, $\tau_{s,1} \approx 100$ ps. Such a strong decrease of $\tau_{s,1}$ at relatively small η , when the spin relaxation from $J=1$ to $J=2$ states with spin flip of the electron or hole remains very slow, is quite surprising. The mechanism is not clear. We attribute this peculiarity to the effect of statistical fluctuations of the Mn magnetic moment. Any random change in magnetic moment during the exciton lifetime alters the exciton wave function, due to $sp-d$ interaction, and leads to energy transfer between the exciton and Mn spin system. This channel appears to be effective for energy relaxation between $J_z=\pm 1$ states with Mn spin system as a reservoir.

V. FINE STRUCTURE AND EMISSION LINE BROADENING OF QD EXCITONS SUBJECTED TO $sp-d$ EXCHANGE INTERACTION WITH Mn ION SPINS

The effect of the magnetic moment of the Mn ion system, \mathbf{m} , on exciton levels in a neutral low-symmetry (C_{2v}) QD is considered in detail in the Appendix. The effect of a fixed magnetic moment is well described in terms of an effective magnetic field that appears in the expressions for exciton energies [formula (A13)]. Magnetic fluctuations are shown to lead to an expected statistical broadening of the exciton level [formula (A19)] and, in addition, to result in a contribution in the transition energy [formula (A18)]. The latter is most important at small magnetic fields $B \parallel Oz$ and in a wide range of in-plane magnetic fields.

A. Faraday geometry

The formulas (A18) and (A19) have been used in Figs. 5 and 6 for the description of experimental exciton transition energies $\langle E \rangle$ and their spectral FWHMs, $\sqrt{8 \ln 2 \langle \delta E^2 \rangle}$, extracted from the emission spectra of QD1 with the smallest penetration of exciton wave function into the magnetic barrier for different excitation densities and various magnetic fields. The lines in these figures show the result of simultaneous approximation of experimental dependences $\langle E \rangle$ and $\sqrt{8 \ln 2 \langle \delta E^2 \rangle}$. The values $\alpha N_0=0.26$ eV, $\beta N_0=-1.11$ eV,²³ $g_X=1.56$,^{17,18} $S_{eff}=1.0$ (Refs. 24 and 25) are taken from the literature. In addition, we put $\eta_e \approx \eta_h = \eta$, as our previous studies of exciton emission from charged QDs in the same CdSe/ZnSe/Zn_{1-x}Mn_xSe structures have shown a small difference in the values of η_e and η_h .²⁶ The values of $T+T_0$, N_{Mn} , η , δ_1 , and w_0^2 have been used as adjustable parameters. The values stated below have been found from an approximation procedure for QD1: $\delta_1 \approx 125$ μ eV, $\eta \approx 0.01$, $N_{Mn} \approx 50$, and the effective temperatures $T+T_0$ are 6.2, 7.3, and 10 K for the three different excitation powers used. The values of $T+T_0$ are in good agreement with the upper estimates of $T \approx 5.7, 6.4,$ and 8.8 K from the ratio of the intensities of two Zeeman components at corresponding excitation densities. The same fitting procedure enables one to determine wave function penetrations for QD2 and QD3 [Fig. 5(c)]. These are $\eta \approx 0.03$ and $\eta \approx 0.04$, respectively.

Figures 5 and 6(a) show that both the transition energies and their spectral widths with nonmonotonic dependence on magnetic field are well described in the whole range of magnetic fields. To show the effect of $e-h$ exchange interaction in asymmetric QDs we display with thin lines in Fig. 6(a) the FWHMs calculated for the set of parameters found from approximation, but neglecting $e-h$ exchange interaction. The qualitative difference in the magnetic field dependence of the linewidth from that in a symmetric QD at low magnetic fields is connected with the mixing of $J_z=+1$ and -1 X states in low-symmetry QDs by the $e-h$ exchange interaction. The exciton states in low-symmetry QDs have no magnetic moment in zero external magnetic field. They interact with fluctuating magnetic moment \mathbf{m} only due to disturbance of the balance between the $J_z=1$ and -1 components in the wave function induced by these fluctuations. As a result the exciton energies have a quadratic dependence on m_z , as shown in Fig. 6(b). Figures 6(b) and 6(c) illustrate the effect of magnetic fluctuations on broadening of the emission lines of bright excitons in symmetric QDs with $\delta_1=0$ and asymmetric ones with $\delta_1 \neq 0$. The same magnetic fluctuations cause much smaller line broadening in the presence of $e-h$ exchange splitting.

A magnetic field $B \parallel Oz$ disturbs the balance between the contributions in the exciton wave function from the $J_z=+1$ and $J_z=-1$ components established by $e-h$ exchange interaction at $B=0$. This leads to increase of the exciton magnetic moment and, hence, to growth of the emission line broadening. The effect of $e-h$ exchange interaction in the QD disappears only when $g\mu_b B$ exceeds the exchange splitting. The exciton emission linewidth decreases at high B due to suppression of longitudinal magnetic fluctuations of Mn ion spin system connected with Mn ion spin alignment.⁷

Using the values of η and $T+T_0$ found above from the fitting procedure one can estimate contributions to the effective g factor according to (A16). The values are $G_{Xz} \approx -7.5$, -9 , and -20 for QD1, QD2, and QD3, respectively.

B. Voigt geometry

Let us now consider the magnetic field dependences of exciton transition energies in the in-plane magnetic field for QD1, which are qualitatively different from those in the Faraday geometry. Figures 2(a) and 5(b) show that the bright components conserve their linear polarization in the magnetic field and demonstrate a very weak change in the energy. The energies of components of the $J=1$ doublet in the in-plane magnetic field are determined by their mixing with dark states separated by ~ 2 meV. Figures 2(a) and 5(b) show that the energy of the $\pi_{y'}$ component is nearly independent of $B \parallel Oy'$. That means that at $B \leq 6$ T the difference $(|g_{hy'}^{eff}| - g_e^{eff})\mu_B B \ll 2$ meV. In contrast, the shift to higher energies of the $\pi_{x'}$ component determined by the ratio $(|g_{hy'}^{eff}| + g_e^{eff})\mu_B B / \Delta$ is well pronounced, which indicates a much higher coupling of the $\pi_{x'}$ bright component with the dark one. This conclusion is supported by the appearance of dark exciton emission with $\pi_{x'}$ polarization (line X_D) in the spectra at $B > 2$ T. Its intensity grows quadratically with B as is expected from formula (A8) due to increased admixture of the $J=1$ exciton state.

Measurements at $B \parallel Ox'$ have shown that properties of QD emission are quite similar to those at $B \parallel Oy'$; namely, only one dark line appears with growth of the magnetic field for both directions of B . It has the same polarization along the Ox' axis. This, according to (A9), indicates that terms $\sim j^3$ in the Hamiltonian (A5) are insignificant and that the hole properties are determined mostly by elastic stress, as in charged QDs.^{26,27}

VI. EFFECT OF CARRIERS ON Mn ION SPIN SYSTEM

It has been shown in Sec. IV that even a relatively small ($\eta \sim 1-4\%$) content of the QD exciton wave function in a DMS barrier has a strong effect on QD exciton transition energies, spin relaxation, and Auger recombination. At the same time, the transition energies are well described in the approximation that the magnetic moment \mathbf{m} of the Mn spin system is not influenced by the sp - d exchange interaction with carriers in the QD exciton or, in other words, the relaxation rate of the Mn spin system in a relatively weak exchange field of QD carriers with small η is markedly smaller than the exciton decay rate.

To estimate the dynamic magnetic polaron (MP) effect in the investigated QDs, let us consider the polarization properties of exciton emission at zero magnetic field. In QDs of high symmetry (D_{2d} and higher), the bright exciton state is twice degenerate with $J_z = \pm 1$, and the MP formation is similar for both of them. The e - h exchange in low-symmetry QDs causes the splitting of these states and makes them unequal. Figure 6(b) shows that only the energy of the lower exciton level decreases with increase of the effective sp - d exchange field $B_{exch,z} \propto |m_z|$. This makes the formation of a magnetic polaron possible only for the low-energy X state.

The average energies of bright exciton transitions for ground and excited states can be written as $\langle E_{G,1} \rangle = E_0 - \sqrt{(\delta_1/2)^2 + E_{fl}^2 + E_{MP}^2}$, $\langle E_{U,1} \rangle = E_0 + \sqrt{(\delta_1/2)^2 + E_{fl}^2}$, where E_0 is the average energy of a bright doublet, δ_1 is the e - h exchange splitting, E_{fl} is the contribution from the fluctuations of \mathbf{m} , and E_{MP} stands for the MP energy.

The presence of finite Mn magnetization in the moment of exciton recombination should lead, according to Eq. (A14), to a partial conversion from linear to circular polarization due to disturbance of the balance between the $J_z = 1$ and -1 contributions to the exciton wave function. Both directions of \mathbf{m} along Oz are equiprobable for magnetic fluctuations. Thereby the magnetic fluctuations and dynamic MP effect cause a decrease of the linear polarization of exciton components but do not result in any circular polarization. The degrees of linear polarization ρ_L measured for QD1 at low excitation density in zero magnetic field [Fig. 4(b)] are equal to 50% and 70% for high-energy and low-energy components, respectively. The larger depolarization of the low-energy component is connected with its additional depolarization due to the dynamic MP effect. Note that the difference in ρ_L for the two components is observed only for the exciton emission. It disappears completely in the emission of a two-exciton state when the magnetic fluctuations influence the exciton energy in the final state of the transition [Fig. 2(a)].

Taking the above values of ρ_L and the X line splitting $\Delta E_X = \langle E_{U,1} \rangle - \langle E_{G,1} \rangle \approx 250 \mu\text{eV}$ at $B=0$, we found $\delta_1 \approx 125 \mu\text{eV}$, $E_{fl} \approx 90 \mu\text{eV}$, and $E_{MP} \approx 130 \mu\text{eV}$. The value of δ_1 complies with that found from the experimental dependences of energies and linewidths in Sec V. Note that the E_{MP} in CdSe/ZnSe/Zn $_{1-x}$ Mn $_x$ Se QDs with $\eta \sim 1\%$ found above is too small to influence the exciton transition energies and the emission linewidths markedly. This justifies the disregard of the MP formation process in the discussion in Sec V. However, this process results in a well-pronounced effect in the exciton emission polarization that allows one to use the polarization measurements for an accurate determination of spin relaxation in the Mn spin system connected with the sp - d exchange interaction between the spins of Mn ions and free carriers in the QD.

VII. SUMMARY

Investigation of the polarized spectra of exciton emission from low-symmetry CdSe/ZnSe/Zn $_{1-x}$ Mn $_x$ Se QDs with a small amount of wave function penetration η into the semi-magnetic layers has made it possible to resolve the fine structure of exciton states caused by the e - h exchange interaction. The penetration of the wave function, η , and the effective number of Mn ions interacting with the exciton wave function have been estimated from the magnetic field dependences of the exciton emission energies and linewidths. The anisotropic e - h exchange interaction in QDs with $\eta \sim 1-4\%$ leads to a marked modification of exciton properties in zero magnetic field; namely, the exciton emission linewidth turns out to be much smaller than it is expected to be in the absence of e - h interaction. This happens due to the mixing of $J_z = +1$ and -1 states, leading to suppression of the effect of magnetic fluctuation on exciton states. The mag-

netic fluctuations and Mn spin alignment induced by carriers in the QD result in a pronounced depolarization of the exciton emission at $B=0$ which allows one to estimate the spin relaxation in the Mn ion system. Even a small value of $\eta \sim 1\%$ leads to considerable acceleration of the relaxation between bright exciton states $J_z = \pm 1$ in a magnetic field $B \parallel O_z$. The exciton spin relaxation time was estimated to be less than 100 ps, while for nonmagnetic CdSe/ZnSe QDs it exceeds 1 ns.²² On the other hand, the nonradiative Auger recombination becomes substantial only when the wave function penetration η reaches a value of $\sim 4\%$. Finally, our measurements have shown that relaxation of bright excitons into dark $J=2$ states, requiring separate spin flips of electron or hole, is negligible in the whole range of $\eta < 4\%$.

ACKNOWLEDGMENTS

The authors are thankful to K. V. Kavokin, A. V. Koudinov, E. L. Ivchenko, A. A. Toropov, and P. S. Dorozhkin for helpful discussions, and S. V. Dubonos for preparation of samples. The work is supported by RFBR and INTAS grants.

APPENDIX: ENERGIES AND WAVE FUNCTIONS OF EXCITONS IN QDs SUBJECTED TO $sp-d$ EXCHANGE INTERACTION WITH Mn IONS

The exciton structure in CdSe/ZnSe/Zn_{1-x}Mn_xSe QDs subjected to $sp-d$ exchange interaction with Mn ion spins without a magnetic polaron is similar to that in nonmagnetic QDs. The set of basis functions is the exterior product of twofold-degenerate conduction-band states φ_e^\pm with spin $s_z = \pm 1/2$ and fourfold-degenerate valence-band hole states with momentum projection $j_z = \pm 1/2, \pm 3/2$. The fine structure is determined by point symmetry in the QD depending on both the semiconductor crystal symmetry and the symmetry of the QD confining potential.^{3,28} Linear polarization of the exciton component along a direction close to $[110]$ indicates that the QD potential symmetry is close to C_{2v} . Studies of charged excitons in QDs in the same samples have shown that the main contribution to the lowering of the QD potential symmetry is connected to a lattice strain.²⁶ Taking into account that fact, the Hamiltonian for exciton states can be written as

$$H = H_{stress} + H_{exch} + H_{magn}, \quad (\text{A1})$$

where the term caused by elastic stress is

$$H_{stress} = \frac{\Delta_{lh}}{2} \left(\frac{1}{4} I - j_z^2 \right) + \frac{\gamma \Delta_{lh}}{\sqrt{3}} (j_x j_y + j_y j_x). \quad (\text{A2})$$

Here the coordinate system is chosen along the cubic crystal axes with O_z parallel to the growth direction, j_i are the momentum projection operators of the valence-band hole, and I stands for the unity operator. The second term in (A2) with dimensionless quantity $\gamma < 1$, corresponding to the ε_{xy} component of the elastic stress tensor, alters ground states.^{26,29} In the first order by γ , they can be written as $\psi_{hh}^+ = | +3/2 \rangle - i\gamma | -1/2 \rangle$ and $\psi_{hh}^- = | -3/2 \rangle + i\gamma | +1/2 \rangle$. Heavy-hole exciton wave functions that are eigen for H_{stress} can be designated as $| \pm 1 \rangle = \psi_{hh}^\pm \varphi_e^\mp$ for bright states and $| \pm 2 \rangle = \psi_{hh}^\pm \varphi_e^\pm$ for dark

states. The mean exciton momentum projections $\langle J_z \rangle$ are equal to $\pm(1-2\gamma^2)$ for bright and $\pm(2-2\gamma^2)$ for dark states.

The influence of the $e-h$ exchange interaction is described by the second term in Eq. (A1):

$$H_{exch} = [a_1(j_x s_x + j_y s_y) + a_z j_z s_z + b_1(j_x^3 s_x + j_y^3 s_y) + b_z j_z^3 s_z] + [a_2(j_x s_y + j_y s_x) + b_2(j_x^3 s_y + j_y^3 s_x)], \quad (\text{A3})$$

where s_i are the electron spin operators and a_i, b_i are exchange constants. The first square bracket in (A3) corresponds to exchange interactions in QDs with D_{2d} symmetry, while the second describes symmetry lowering down to C_{2v} . The exchange interaction splits excitonic states and leads also to the admixture of light-hole exciton states into the heavy-hole ones. The latter is of the order of $(|a|+|b|)/\Delta_{lh}$ and can be safely neglected at $\Delta_{lh} > 10$ meV. In this approximation, the heavy-hole exciton energies and wave functions can be written as

$$E_{1,2} = \delta_0/2 \pm \delta_1/2, \quad \Psi_{1,2} = (| +1 \rangle \pm i | -1 \rangle) / \sqrt{2},$$

$$E_{3,4} = \delta_0/2 \pm \delta_2/2, \quad \Psi_{3,4} = (| +2 \rangle \mp | -2 \rangle) / \sqrt{2}. \quad (\text{A4})$$

Here the splitting constants are $\delta_0 = -\frac{3}{8}(4a_z + 9b_z)$, $\delta_1 = -\frac{1}{2}[3b_2 + \sqrt{3}(4a_1 + 7b_1)\gamma]$, $\delta_2 = \frac{1}{2}[3b_1 + \sqrt{3}(4a_2 + 7b_2)\gamma]$.

Emission from the bright states Ψ_1 and Ψ_2 is completely linearly polarized along $\vec{e}_{x'} = (1/\sqrt{2})(\vec{e}_x + \vec{e}_y)$ and $\vec{e}_{y'} = (1/\sqrt{2}) \times (\vec{e}_x - \vec{e}_y)$ directions, respectively. Optical transition from the Ψ_3 state is forbidden in the dipole approximation, while the Ψ_4 state has a dipole moment along \vec{e}_z proportional to $\sim \gamma^2$.

The effect of a magnetic field on exciton energies in nonmagnetic QDs of C_{2v} symmetry is described by the Hamiltonian

$$H_{magn} = \mu_B g_e (\vec{s}, \vec{B}) + 2\mu_B \sum_{i=(x',y',z)} (\kappa_j i + q_j i^3) B_i, \quad (\text{A5})$$

where μ_B is the Bohr magneton, g_e is the electron g factor, and the constants κ and q describe the interaction of the hole with magnetic field.²⁸

A magnetic field $B \parallel O_z$ (Faraday geometry) does not lower the QD symmetry and, hence, does not mix bright and dark states. The coupling with the light-hole states is also very small, and the Hamiltonian reduces to 2×2 eigenvalue problems. The solution has the following form:

$$E_{1,2} = \frac{1}{2} (\delta_0 \pm \sqrt{\delta_1^2 + \mu_B^2 g_{x_z}^2 B_z^2}),$$

$$\Psi_{1,2} = L_{1,2} (| +1 \rangle, | -1 \rangle),$$

$$E_{3,4} = \frac{1}{2} (\delta_0 \pm \sqrt{\delta_2^2 + \mu_B^2 g_{x_z}^2 B_z^2}),$$

$$\Psi_{3,4} = L_{3,4} (| +2 \rangle, | -2 \rangle). \quad (\text{A6})$$

The hole g factor is introduced by the relation $g_{hz} = \frac{1}{2}(12\kappa_z + 27q_z)$, $g_{xz} = g_{hz} - g_e$, and L_i are linear functions with coefficients depending on external field and splitting constants δ_i . The magnetic field B_z changes the linear polarization of the bright exciton emission into circular polarization and the de-

gree of linear polarization $\rho_L = |(I_{x'} - I_{y'}) / (I_{x'} + I_{y'})|$ decreases with increasing B_z as

$$\rho_L = \delta_1^2 / \sqrt{\delta_1^2 + \mu_B^2 g_{Xz}^2 B_z^2}. \quad (\text{A7})$$

In Voigt geometry, $B \perp Oz$ lowers the QD symmetry and mixes dark and bright states. For the magnetic field along the principal axes of QD symmetry the problem can be treated analytically. At $\delta_0 \gg \delta_1, \delta_2$, the intensity $I_{i,x'(y')}$ of the dipole transition for the i th dark state polarized along Ox' (Oy') can be written as

$$I_{3,x'(y')} \propto \mu_B^2 (g_{hx'(y')} \pm g_e)^2 B_{x'(y')}^2 \frac{|1 \pm 2\gamma/\sqrt{3}|}{4\delta_0^2},$$

$$I_{4,x'(y')} \propto \mu_B^2 (g_{hy'(x')} \pm g_e)^2 B_{y'(x')}^2 \frac{|1 \pm 2\gamma/\sqrt{3}|}{4\delta_0^2}, \quad (\text{A8})$$

where the lower sign corresponds to the index in parentheses, and the in-plane hole g factor depends on the magnetic field direction:

$$g_{hx'} = \sqrt{3}\gamma(4\kappa_{x'} + 7q_{x'}) + 3q_{x'},$$

$$g_{hy'} = \sqrt{3}\gamma(4\kappa_{y'} + 7q_{y'}) - 3q_{y'}. \quad (\text{A9})$$

The mixing of bright and dark states does not change the polarization properties of emission of bright X states, but gives the oscillator strength $I \sim B^2$, with the polarization of the admixed bright state, to the dark ones.

The penetration of the exciton wave function into the DMS barrier leads to an additional sp - d exchange interaction, of electrons (e) and holes (h) with magnetic ions described by the Hamiltonians

$$H_{exch}^e = \alpha \sum_n \int \vec{\sigma} \vec{S}_n |\psi_e(\vec{r})|^2 \delta(\vec{r} - \vec{R}_n) d^3\vec{r}, \quad (\text{A10})$$

$$H_{exch}^h = \beta \sum_n \int \vec{J} \vec{S}_n |\psi_h(\vec{r})|^2 \delta(\vec{r} - \vec{R}_n) d^3\vec{r}, \quad (\text{A11})$$

where S_n is the spin operator of magnetic ions with the position vector \vec{R}_n , and $\alpha(\beta)$, ψ_i , and r are the electron (hole) exchange integral, wave function, and position vector, respectively.

In DMS semiconductors, the sp - d exchange interaction leads to the formation of exciton magnetic polarons due to alignment of Mn ion spins along the exciton spin. As was found in Sec. IV, this effect can be neglected in emission spectra of CdSe/ZnSe/Zn $_{1-x}$ Mn $_x$ Se QDs with an introduced ZnSe barrier of ~ 1.75 nm recorded under cw excitation because of the long exciton magnetic polaron formation time compared to the exciton lifetime. In this case, the average Mn ion spin $\langle \vec{S} \rangle$ is completely determined by the external magnetic field. As the Mn spin system in a DMS is paramagnetic, $\langle \vec{S} \rangle$ is parallel to \vec{B} and equal to zero at $B=0$. However, the effect of the sp - d exchange interaction on the emission spectra does not vanish even at $B=0$ because of statistical Mn moment fluctuations that manifest themselves mostly in

the spectral width of emission. A magnetic field leads to spin alignment of Mn spins and, hence, macroscopic magnetization $\vec{M} = -xN_0\mu_B g_{Mn} \langle \vec{S} \rangle$. It can be described by a modified Brillouin function $\text{Br}_{5/2}(y)$:

$$\vec{M} = xN_0 S_{eff} \mu_B g_{Mn} \text{Br}_{5/2} \left(\frac{\mu_B g_{Mn} S B}{k_b(T + T_0)} \right) \frac{\vec{B}}{B}, \quad (\text{A12})$$

where x is the Mn concentration, N_0 is the number of cations per unit volume, and $g_{Mn}=2$ is the g factor of Mn $^{2+}$.²³ The effective Mn spin $S_{eff} < S=5/2$, and the effective temperature $T_{eff}=T+T_0$ takes into account the antiferromagnetic interaction between neighboring Mn ion spins.

In the studied structures only part $\eta_{e(h)}$ of the electron (hole) wave function penetrates into the DMS barrier, where it decays exponentially. Thus the effective sp - d interaction takes place only with a limited quantity $N_{Mn}=N_0V_{loc}x$ of Mn ions in the exciton localization volume V_{loc} with mean magnetic moment $\langle \vec{m} \rangle = V_{loc} \vec{M}$. The whole process can be viewed as follows: The electron (hole) in the QD interacts with N_{Mn} ions, but the magnitude of interaction is modified by a factor $\eta_{e(h)}$, because only part $\eta_{e(h)}$ of the $e(h)$ wave function overlaps with the manganese ions. The value of Zeeman splitting is determined by $\eta_{e(h)}$ only. On the other hand, the linewidths depend also on N_{Mn} , which is determined by the spatial decay rate of the carrier wave functions in the DMS layer.

The effect of \vec{m} on electron (hole) states is similar to that of the magnetic field and can be easily taken into account by the following terms in the Hamiltonian: $(\alpha\eta_e/g_{Mn}\mu_B V_{loc}) \times (\vec{s}, \vec{m})$, $(\beta\eta_h/3g_{Mn}\mu_B V_{loc})(\vec{j}, \vec{m})$ for the electron and hole, respectively. These terms have the same structure as the Zeeman ones in (A5). The energy and degree of linear polarization of the bright exciton in Faraday geometry can now be written as

$$E_{1,2} = \frac{1}{2} [\delta_0 \pm \sqrt{\delta_1^2 + (\mu_B g_{Xz} B_z + C m_z)^2}] \quad (\text{A13})$$

$$\rho_L = \delta_1^2 / \sqrt{\delta_1^2 + (\mu_B g_{Xz} B_z + C m_z)^2}, \quad (\text{A14})$$

where $C = (\beta\eta_h - \alpha\eta_e)N_0x/g_{Mn}\mu_B N_{Mn}$.

In the limit of low magnetic fields, the transition energies for the bright doublet $E_{X,\pm 1} = \frac{1}{2} \{ \delta_0 \pm \sqrt{\delta_1^2 + \mu_B^2 [g_{Xz} + G_{Xz} f(B_z, T)]^2 B_z^2} \}$ can be described using the effective g factor

$$g_{e(h)}^{eff} = g_{e(h)} + G_{e(h)}. \quad (\text{A15})$$

Here G_i stand for the contribution from the sp - d interaction,

$$G_{ez} = \frac{7x\alpha g_{Mn} \eta_e S_{eff}}{6k_b(T + T_0)}, \quad G_{hz} = \frac{7x\beta g_{Mn} \eta_h S_{eff}}{6k_b(T + T_0)},$$

$$G_{Xz} = G_{hz} - G_{ez}, \quad (\text{A16})$$

and the function f reflects the dependence of the Mn moment on magnetic field. This function is chosen so that $\lim_{B_z \rightarrow 0} f(B_z, T) = 1$. At high $B \parallel Oz$, it decreases as $1/B_z$ due to the saturation of M .

The statistical fluctuations of \vec{m} at $N_{Mn} \gg 1$ can be treated thermodynamically, considering \vec{m} as a Gaussian random

quantity. The dispersion of the projection m_{\parallel} parallel to the external magnetic field can be expressed via dependence of the average magnetization on B as

$$\langle \delta m_{\parallel}^2 \rangle = \frac{d\langle m_{\parallel} \rangle}{dB} k_b (T + T_0). \quad (\text{A17})$$

In Faraday geometry, the exciton energy dependence $E(\vec{B}, \vec{m})$ on the in-plane magnetic field can be neglected; thus fluctuations of \vec{m} perpendicular to B are also not essential. In this case, the average transition energy $\langle E \rangle$ and its dispersion $\langle E^2 \rangle$ are equal to

$$\langle E \rangle = \int E(B_z, m_z) \rho(m_z, \langle m_z \rangle, \langle \delta m_z^2 \rangle) dm_z \quad (\text{A18})$$

$$\begin{aligned} \langle \delta E^2 \rangle = & \int E^2(B_z, m_z) \rho(m_z, \langle m_z \rangle, \langle \delta m_z^2 \rangle) dm_z \\ & - \left(\int E(B_z, m_z) \rho(m_z, \langle m_z \rangle, \langle \delta m_z^2 \rangle) dm_z \right)^2 + w_0^2, \end{aligned} \quad (\text{A19})$$

where $E(B_z, m_z)$ is given by (A13), $\rho(m_z, \langle m_z \rangle, \delta m_z^2)$ is the Gaussian distribution of m_z with average $\langle m_z \rangle = N_{\text{Mn}} M / (N_0 x)$ and dispersion $\langle \delta m_z^2 \rangle$, according to (A12) and (A17), and w_0^2 takes into account all factors causing spectral broadening other than magnetic fluctuations.

-
- ¹J. Y. Marzin, J. M. Gérard, A. Izraël, D. Barrier, and G. Bastard, *Phys. Rev. Lett.* **73**, 716 (1994).
- ²D. Gammon, E. S. Snow, B. V. Shanabrook, D. S. Katzer, and D. Park, *Phys. Rev. Lett.* **76**, 3005 (1996).
- ³M. Bayer *et al.*, *Phys. Rev. B* **65**, 195315 (2002).
- ⁴B. Urbaszek, R. J. Warburton, K. Karrai, B. D. Gerardot, P. M. Petroff, and J. M. Garcia, *Phys. Rev. Lett.* **90**, 247403 (2003).
- ⁵A. A. Maksimov, G. Bacher, A. McDonald, V. D. Kulakovskii, A. Forchel, C. R. Becker, G. Landwehr, and L. W. Molenkamp, *Phys. Rev. B* **62**, R7767 (2000).
- ⁶J. Seufert, G. Bacher, M. Scheibner, A. Forchel, S. Lee, M. Dobrowolska, and J. K. Furdyna, *Phys. Rev. Lett.* **88**, 027402 (2001).
- ⁷G. Bacher *et al.*, *Phys. Rev. Lett.* **89**, 127201 (2002).
- ⁸P. S. Dorozhkin *et al.*, *Phys. Rev. B* **68**, 195313 (2003).
- ⁹A. V. Chernenko, P. S. Dorozhkin, V. D. Kulakovskii, A. S. Brichkin, S. V. Ivanov, and A. A. Toropov, *Phys. Rev. B* **72**, 045302 (2005).
- ¹⁰M. Nawrocki, Y. G. Rubo, J. P. Lascaray, and D. Coquillat, *Phys. Rev. B* **52**, R2241 (1995).
- ¹¹L. Besombes, Y. Leger, L. Maingault, D. Ferrand, H. Mariette, and J. Cibert, *Phys. Rev. Lett.* **93**, 207403 (2004).
- ¹²Y. Leger, L. Besombes, L. Maingault, D. Ferrand, and H. Mariette, *Phys. Rev. B* **72**, 241309 (2005).
- ¹³A. K. Bhattacharjee and C. Benoit à la Guillaume, *Phys. Rev. B* **55**, 10613 (1997).
- ¹⁴I. I. Reshina, S. V. Ivanov, D. N. Mirlin, A. A. Toropov, A. Waag, and G. Landwehr, *Phys. Rev. B* **64**, 035303 (2001).
- ¹⁵M. Keim *et al.*, *J. Appl. Phys.* **88**, 7051 (2000).
- ¹⁶The value of η depends on the nonmagnetic barrier thickness and cannot be measured directly. Therefore it was estimated from the splitting of exciton levels at high magnetic fields normal to the QD plane that is sufficient for the alignment of Mn ion spins. In these fields, $\eta = \delta_{QD} / \delta_{bulk}$, where δ_{QD} and δ_{bulk} are the exciton splittings induced by an sp - d exchange interaction in the QD and bulk with similar Mn content, respectively; $\delta_{bulk} = (\alpha - \beta) N_0 x S_{eff} = 150$ meV at $x = 0.11$ (Refs. 25 and 23).
- ¹⁷V. D. Kulakovskii, G. Bacher, R. Weigand, T. Kümmell, A. Forchel, E. Borovitskaya, K. Leonardi, and D. Hommel, *Phys. Rev. Lett.* **82**, 1780 (1999).
- ¹⁸J. Puls, M. Rabe, H.-J. Wünsche, and F. Henneberger, *Phys. Rev. B* **60**, R16303 (1999).
- ¹⁹The order of the σ^+ and σ^- components is determined by the sign of the difference in g factors, $g_h - g_e$. In nonmagnetic QDs it is positive. The exchange constant for the conduction band is positive, while it is negative for the valence band. Thus introduction of Mn ions increases g_e and decreases g_h , and $g_h - g_e$ eventually changes its sign.
- ²⁰S. Cortez, O. Krebs, S. Laurent, M. Senes, X. Marie, P. Voisin, R. Ferreira, G. Bastard, J.-M. Gérard, and T. Amand, *Phys. Rev. Lett.* **89**, 207401 (2002).
- ²¹G. Bacher, R. Weigand, J. Seufert, V. D. Kulakovskii, N. A. Gippius, A. Forchel, K. Leonardi, and D. Hommel, *Phys. Rev. Lett.* **83**, 4417 (1999).
- ²²V. D. Kulakovskii, R. Weigand, G. Bacher, J. Seufert, T. Kümmell, A. Forchel, K. Leonardi, and D. Hommel, *Phys. Status Solidi A* **178**, 323 (2000).
- ²³J. K. Furdyna, *J. Appl. Phys.* **64**, R29 (1988).
- ²⁴W. J. Ossau and B. Kuhn-Heinrich, *Physica B* **184**, 422 (1993).
- ²⁵D. Keller, D. R. Yakovlev, B. König, W. Ossau, T. Gruber, A. Waag, L. W. Molenkamp, and A. V. Scherbakov, *Phys. Rev. B* **65**, 035313 (2001).
- ²⁶A. S. Brichkin, A. V. Chernenko, E. A. Chekhovich, P. S. Dorozhkin, V. D. Kulakovskii, S. V. Ivanov, and A. A. Toropov, *JETP* **132**, 426 (2007).
- ²⁷The conclusion about the insignificant role of the $\sim j^3$ term in investigated CdSe/ZnSe QDs is opposite to that made by Kowalik *et al.* recently from studies of CdTe/ZnTe QDs (Ref. 30). Our data are in agreement with earlier results for nonmagnetic CdSe/ZnSe QDs (Ref. 29). The different role of various terms in the Hamiltonian can be connected with differences in the shape and strain distribution in CdSe/ZnSe and CdTe/ZnTe QDs. The exact answer requires further investigation.
- ²⁸H. W. van Kesteren, E. C. Cosman, W. A. J. A. van der Poel, and C. T. Foxon, *Phys. Rev. B* **41**, 5283 (1990).
- ²⁹A. V. Koudinov, I. A. Akimov, Y. G. Kusrayev, and F. Henneberger, *Phys. Rev. B* **70**, 241305 (2004).
- ³⁰K. Kowalik, O. Krebs, A. Golnik, J. Suffczynski, P. Wojnar, J. Kossut, J. A. Gaj, and P. Voisin, *Phys. Rev. B* **75**, 195340 (2007).